Grass Research

ARTICLE

Open Access

https://doi.org/10.48130/grares-0025-0016

Grass Research **2025**, 5: e019

Rhizosphere and root-associated microbial community structures and plant physiology responses to Large Patch disease in zoysiagrass

Xie Zheng[1,2], Huaiyong Tang[1,2], Hongjian Wei[1,2], Wen Liu[1,2] and Tianzeng Liu[1,2*]

[1] *College of Forestry and Landscape Architecture, South China Agricultural University, Guangzhou 510642, China*
[2] *Guangdong Engineering Research Center for Grassland Science, Guangzhou 510642, China*
* Corresponding author, E-mail: liutianzeng@scau.edu.cn

Abstract

Large Patch disease caused by *Rhizoctonia solani* devastates zoysiagrass turf, yet its microbiome-mediated pathogenesis remains elusive. This study investigated the effects of *R. solani* strain ZS-1 on zoysiagrass physiology and rhizosphere microbial communities. Pathogen inoculation significantly inhibited plant growth ($p < 0.05$), reducing net photosynthetic rate (32.1%), chlorophyll content (19.4%), and photochemical efficiency (Fv/Fm). Concurrently, the antioxidant defense was activated, with catalase (CAT), and phenylalanine ammonia-lyase (PAL) activities increasing by 2.1- and 3.3-fold, respectively. Furthermore, soil nutrient dynamics shifted, showing a 40% decline in available nitrogen and 22% increase in phosphorus. Integrating 16S/ITS amplicon sequencing with physiological assays, we decoupled tripartite interactions among pathogen invasion, microbiome restructuring (n = 3 biological replicates), and host responses. The results showed that the bacterial Chao1 index increased significantly while the Shannon index declined. Key microbial shifts included declines in Ascomycota and Basidiomycota fungi and enrichment of Actinobacteria and Chloroflexi in the rhizosphere. Dominant bacterial genera such as *Geobacter* and *Anaerolinea* were linked to enhanced nutrient cycling and stress tolerance. Soil properties, including available potassium and phosphorus, correlated with specific microbial taxa, such as Glomeromycota, suggesting their role in nutrient modulation under pathogen stress. These findings highlight the complex interplay between *R. solani* invasion, microbial community restructuring, and zoysiagrass physiological responses. This study provides foundational insights into leveraging soil microbiome management to improve zoysiagrass resilience against Large Patch disease, offering practical strategies for sustainable turfgrass cultivation.

Citation: Zheng X, Tang H, Wei H, Liu W, Liu T. 2025. Rhizosphere and root-associated microbial community structures and plant physiology responses to Large Patch disease in zoysiagrass. *Grass Research* 5: e019 https://doi.org/10.48130/grares-0025-0016

Introduction

Zoysiagrass (*Zoysia* spp.) is a warm-season (C4) turfgrass that enjoys popularity in the transition zone of China[1]. Some desirable traits of zoysiagrass include its high density and resistance to pests. Moreover, zoysiagrass demands lower quantities of fertilizers and pesticides compared to certain cool-season turfgrass species like creeping bentgrass *(Agrostis stolonifera* L.)[2].

Large Patch disease, caused by *Rhizoctonia solani* AG 2-2 LP, stands as the most prevalent and severe ailment afflicting zoysiagrass within the transition zone and wherever zoysiagrass is cultivated. This ailment can result in extensive swaths of withered turf during the spring and fall seasons. Characteristic symptoms include sunken light brown-to-straw patches, frequently bordered by bright orange margins[3]. These patches can span up to 6 m or more in diameter, sometimes interspersed with healthy zoysiagrass. In summer conditions, the emergence of new shoots from viable stolons and rhizomes often leads to a full recovery. Studies in China have also indicated that Large Patch disease proliferates most rapidly when the temperature hovers around 30 °C and the environment maintains a relative level of humidity[4]. When the ailment manifests, grass leaves develop water-soaked rot or yellow spots, with severe cases resulting in the rapid formation of dead patches. Effectively controlling and preventing this disease poses considerable challenges, rendering it a significant hurdle in lawn maintenance and management[5]. No prior studies have systematically deciphered the coordinated responses of the rhizosphere-root endosphere microbiota in zoysiagrass under *R. solani* infection.

As the primary plant organs, roots are fundamentally tasked with nutrient and water acquisition from the soil substrate. Additionally, roots play a significant role in the secretion of various chemicals and nutrients into the rhizosphere soil, referred to as the rhizosphere. This phenomenon attracts a diverse array of microorganisms, including bacteria, fungi, algae, and protozoa, which coexist alongside plant roots[6]. Both biotic stressors (e.g., pathogen attack) and abiotic stressors (e.g., soil salinity) exert selective pressures reshaping rhizosphere microbiome assembly. Microbes can detect signal molecules emitted by plants, resulting in either an increase or decrease in specific microbial populations[7]. Conversely, rhizosphere-associated microbes are actively engaged in a range of metabolic processes, imparting various positive effects on plant growth and their ability to adapt to biotic and abiotic stresses[8]. Given the critical role of rhizosphere microbiota in plant stress responses, their potential interplay with pathogens like *Rhizoctonia solani* requires systematic exploration.

Over the past decade, numerous studies have surfaced, highlighting the beneficial role of plant growth-promoting rhizobacteria (PGPR) in enhancing stress tolerance in plants. These PGPR members employ diverse mechanisms, such as establishing a protective buffer zone for plants against stresses, producing various plant growth-promoting hormones, and inducing systemic resistance in plants[9–11]. Furthermore, microbes influence factors like soil pH, soil structure, nutrient mineralization, and soil fertility, which can partially impact plant survival and stress response. Consequently, rhizosphere-associated microbes play a pivotal role in augmenting Zoysiagrass stress tolerance. Additionally, endophytic microorganisms can function as beneficial bacteria and induce resistance to pathogens. Research has demonstrated that during the initial stages of interaction between Zoysiagrass and endophytic microorganisms, these microorganisms can elicit an immune response in

Zoysiagrass, akin to Zoysiagrass' response to pathogens. Subsequently, endophytic microorganisms can evade its immune response through recognition and colonization of Zoysiagrass roots, fortifying its immune system and providing resistance when pathogens invade[12]. It is imperative to conduct further investigations into the colonization and proliferation of the microbial community, along with the community structure of endophytic microorganisms. This research will facilitate the identification and selection of beneficial microbes to enhance zoysiagrass' resistance to Large Patch disease.

Given the knowledge gap in tripartite interactions among *R. solani*, zoysiagrass, and associated microbiomes, it becomes imperative to investigate how these interactions relate to the growth and physiological alterations in zoysiagrass. This understanding is essential for unraveling the mechanisms underlying zoysiagrass tolerance. In our study, we investigated the effects of *Rhizoctonia solani* on zoysiagrass growth and physiological changes, as well as the diversity of root and rhizosphere microbes. We accomplished this through statistical analysis and the sequencing of 16S rDNA and ITS amplicons. Our multifaceted analyses were designed to assess how *Rhizoctonia solani* influences the makeup of zoysiagrass's rhizosphere and inter-rhizosphere microbial communities, to shed new light on this complex relationship.

This study investigates (a) how *Rhizoctonia solani* infection restructures root-associated microbial communities in Zoysiagrass, and (b) whether these microbial shifts correlate with disease susceptibility or resilience phenotypes.

Materials and methods

Preparation of pathogen inoculum

The *Rhizoctonia solani* ZS-1 strain utilized in this study was isolated from a lawn area planted with 'Lanyin No. III' zoysiagrass (*Zoysia japonica* cv. Lanyin No. III) at the Large Patch experimental site of the Teaching and Research Base within South China Agricultural University, Guangzhou, China (latitude 23°30'15'' N, longitude 113°80'21" E). Our research group identified this strain through sequence comparisons of the 16S rRNA and gyrase subunit B gene regions. Subsequently, we deposited the strain at the Guangdong Engineering Research Center for Grassland Science, South China Agricultural University, Guangzhou, China. The procedure for preparing the pathogenic inoculum followed the protocol outlined in Lee et al.[13]. Initially, 20 g of wheat seeds were soaked in a beaker containing sterile water for 24 h. The hydrated wheat seeds were autoclaved at 121 °C for 2 h, followed by aseptic drying under a laminar flow hood. The sterilized wheat seeds were then evenly spread on ZS-1 plates that had been cultured for 3 d. Subsequently, these wheat seeds were placed in an intelligent artificial climate chamber maintained at a temperature of 30 °C. After 7 d of incubation, the wheat grains were removed and ground in a mortar to obtain the pathogenic inoculum.

Plant materials and inoculation treatment

Zoysiagrass (cultivar 'Lanyin No. III') seeds were procured from the International Grass Industry Co. Ltd. located in Tianjin, China. To ensure sterility, the seeds were surface-sterilized by immersing them in 75% ethanol for 5 min, followed by four washes with sterile distilled water. Following surface sterilization, seeds were sown in pre-sterilized plastic pots (10 cm in diameter, 10 cm in height) at a seeding rate of 20 g·m^{-2}, using a substrate mixture of peat and sand in a 3:1 volume ratio. The plastic pots underwent sterilization at 121 °C for 1 h in an autoclave on three consecutive days before initiating the experiment. The potted seedlings were cultivated in a growth chamber under controlled conditions, maintaining a temperature of 30/27 °C, 60% relative humidity, a 14-h light/10-h dark cycle, and photosynthetic active radiation (PAR) of 650 μmol·m^{-2}·s^{-1}. Initially, the pots were watered both in the morning and evening to maintain soil moisture. After seedling emergence, plants received daily watering until excess water drained from the pot bottoms to sustain soil moisture, and they were fertilized once a week with a half-strength Hoagland's solution.

Following 28 d of seedling growth, 0.2 g of pathogenic inoculum was placed near the root system for inoculation (LP). Control plants were inoculated with sterile water (HP). Three replicates of each treatment were employed to monitor disease development on plant leaves in response to the inoculated pathogen for 7 d. Disease severity was assessed by recording the number and severity of affected leaves, calculating disease incidence and the disease index, and applying a turf quality rating system. Subsequently, pathogenic bacteria were re-isolated from the affected areas to confirm that they were the same as those initially inoculated. The day of *Rhizoctonia solani* ZS-1 inoculation of plants was designated as day 0. After 12 d post-inoculation, measurements were taken for root and shoot dry plant weights, and plant samples were collected for further analysis.

Physiological and morphological analyses

To assess the health and overall performance of zoysiagrass, we utilized a turf quality rating system. This system assigns scores on a scale ranging from 1 to 9 based on various criteria, including color, uniformity of the grass canopy, and overall density. On this scale, a score of 1 indicates completely brown and desiccated plants, while a score of 9 signifies a lush, green, and densely populated canopy. A score of 6 represents the minimum acceptable level of turf quality.

The leaf net photosynthetic rate (Pn) was determined using the method outlined by Burgess & Huang[14]. Six fully expanded second leaves located on the upper part of stolons were carefully placed within a 6 cm^2 cuvette chamber connected to a portable infrared gas analyzer, Li-COR 6400 (LI-COR Inc., Lincoln, NE, USA). Within the leaf chamber, leaf Pn was measured under red and blue light sources with an intensity of 800 μmol photon m^{-2}·s^{-1} and a flow rate of 500 μmol·s^{-1}. The leaf area was promptly measured using a handheld digital scanner immediately after the leaf was removed from the cuvette.

To assess chlorophyll fluorescence in the middle section of the first leaf from each seedling, collected at 25 °C, we employed a chlorophyll fluorometer imaging-PAM (Walz, Effeltrich, Germany). Following a 20-min adaptation period in the dark, chlorophyll fluorescence was recorded in the plant samples. The intensities of the saturating and actinic lights were set at 7,200 and 185 μmol photon m^{-2}·s^{-1} PAR (photosynthetic active radiation), respectively. Following the protocol described by Murchie & Lawson[15], we measured the maximum quantum yield of PSII (Fv/Fm), and the photosystem II Efficiency (ΦPSII). Parameters qP and qN were calculated using the equations provided below. Chlorophyll fluorescence parameters were assessed for three sets of leaf samples (four leaf samples from each set) taken from each pot on the day before harvest.

$$qP = (F'm - Fs)/(F'm - F'0) \quad (1)$$

$$qN = (Fm - F'm)/F'm \quad (2)$$

where Fm and F'0 represent maximum and minimum fluorescence intensities of leaf samples adapted to darkness for a 30-min period; F'm is the maximum fluorescence of the light-adapted leaf samples, and Fs is real-time fluorescence of leaves.

To extract chlorophyll from freshly collected leaf samples (1 g), we suspended the leaves in 80% acetone (5 mL v/v). Subsequently, we

employed a spectrophotometer (UV-2800, Unico, Shanghai, China) to measure the optical density (OD) of the extract at three wavelengths: 470, 646, and 663 nm. Carotenoid and chlorophyll levels were quantified using the equations described in Lichtenthaler & Wellburn[16].

Relevant oxidation indexes were measured using commercial kits (Comin, Suzhou, China) for malondialdehyde (MDA), peroxidase (POD), catalase (CAT), and superoxide dismutase (SOD), phenylalanine ammonia-lyase (PAL), Chitinase, and β-1,3-glucanase. All assays were carried out in accordance with the manufacturer's standard protocols. The method described by Gao et al.[17] was used to assess electrolyte leakage (EL) in the leaves.

Determination of soil properties

Soil total phosphorus (TP) was analyzed by $HClO_4$-H_2SO_4 digestion and measured using the molybdate-blue colorimetric method. $NaHCO_3$ (0.5 M) was adopted to extract available phosphorus (AP), and measured using spectrophotometry (UV-5200, Metash Inc., Shanghai, China) at 700 nm. Meanwhile, the Kjeldahl digestion method was utilized to analyze total nitrogen (TN). The KCl extraction-indophenol blue colorimetry was adopted for determining AN[18]. In addition, 1 M NH_4OAc was utilized to extract available potassium (AK), followed by quantification by flame atomic absorption spectroscopy (FP6432, Jingke Inc., Shanghai, China), and $K_2Cr_2O_7$ + H_2SO_4 digestion was applied to determine soil organic carbon (SOC), with the addition of $HgSO_4$ to prevent Cl^- interference[19]. All soil properties were measured in triplicate per sample to ensure data reliability.

DNA extraction and High-Throughput Sequencing (HTS)

At the end of the disease stress treatments, we collected rhizosphere soil and root samples as follows: the plants were gathered and gently shaken to remove loosely adhered soil. Subsequently, rhizosphere soil samples were collected by carefully brushing off the remaining soil using a fine sterile brush. Root samples were gently rinsed multiple times with tap water, followed by washing with sterile water, and then tapped dried on sterilized filter paper. These collected rhizosphere soil and root samples were stored at −80 °C for DNA extraction. Total DNA was isolated separately from approximately 0.5 g of rhizosphere soils and 0.1 g of roots using the Soil DNA Kit (OMEGA, Shanghai, China) and the plant DNA kit (Tiangen, Beijing, China), following the manufacturer's protocols. DNA quality was assessed using a Qubit Fluorometer with the Qubit dsDNA BR Assay kit (Invitrogen, Waltham, MA, USA), and 0.1% agarose gel electrophoresis was utilized to confirm the quality. All extracts were stored at −20 °C. The V3–V4 region of the bacterial 16S ribosomal RNA gene was amplified by PCR using specific primers: 338F (5'-barcode-ACTCCTACGGGAGGCAGCA-3') and 806R (5'-GGACTACH VGGGTWTCTAAT-3'), where the barcode is a unique eight-base sequence for each sample. For fungal community analysis, rDNA-ITS genes were amplified by PCR using primers ITS1F (5'-barcodeCTTG GTCATTTAGAGGAAGTAA-3')/2043R (5'-GCTGCGTTCTTCATCGATGC-3'). PCR was conducted in triplicate in 20-μL reaction mixtures containing 4 μL of 5× FastPfu Buffer, 2 μL of 2.5 mmol dNTPs, 0.8 μL of each primer (5 μmol), 0.4 μL FastPfu Polymerase, 10 ng of template DNA, and ddH_2O to reach a final volume of 20 μL. After amplification, the products underwent recovery and purification, and fluorescence intensity was quantified before constructing a sequencing library using the NEBNext Ultra II DNA Library Prep Kit for Illumina (New England Biolabs, Ipswich, MA, USA). Finally, paired-end sequencing (2 × 250 bp) was carried out on the Illumina HiSeq platform at Guangdong Magigene Biotechnology Co., Ltd. in Guangzhou, China.

Bioinformatics analysis

Processing of the sequencing data involved the use of QIIME software (Quantitative Insights into Microbial Ecology, v1.8.0, http://qiime.org/) following the methodology outlined by Caporaso et al.[20]. This process included filtering for high-quality clean tags, specifically sequences with lengths ≥ 160 bp, and the removal of fuzzy bases. Sequences with more than eight continuous identical bases and those with more than one mismatch in the 5′-primer were also excluded. Subsequently, Usearch (v5.2.236, www.drive5.com/usearch) was employed to check for and eliminate chimeric sequences, resulting in the retention of the desired sequences. The clustering of operational taxonomic units (OTUs) was performed at a similarity level of 97%. For each treatment, the presence of OTUs across three biological replicates was summed to generate the final OTU table. Following the clustering analysis, classification of the OTUs for bacteria was carried out using the Silva databases[21].

Statistical analysis

Data were organized and analyzed using Microsoft Excel 2019. For statistical analyses related to the effects of treatments on zoysiagrass plant physiology, we utilized SPSS 22.0 (SPSS Inc., Chicago, IL, USA). Our analysis involved the application of one-way and two-way ANOVAs, along with Fisher's LSD test, to assess significant differences ($p < 0.05$) in plant physiology indicators between treatments. Relative abundance maps, highlighting bacteria with mean relative abundances greater than 1%, were generated using Origin 8.0 software. Subsequently, we conducted LEfSe (Linear discriminant analysis Effect Size) analysis to analyze relative general abundances. This analysis was performed using the Galaxy online analysis platform (http://huttenhower.sph.harvard.edu/galaxy/). For further analysis, we utilized the R Project (v4.1.3) ggplot2[22] package and employed the Bray-Curtis distance metric to conduct principal coordinate analysis (PCoA). To visualize β-diversity, we used the phyloseq[23] package. Additionally, redundancy analysis (RDA) was carried out, and RDA diagrams were generated using the R (v4.1.3) ggplot2, and vegan[24] packages.

Results

Strain identification

A pathogenic fungal strain, designated as ZS-1, was successfully isolated from a diseased zoysiagrass sample. In the initial stages of growth on the PDA medium, the ZS-1 strain exhibited colorless hyphae that extended outward. By the 5th day of cultivation, the hyphae changed in color from colorless to light yellow, and a small amount of aerial mycelium emerged on the colony's surface. On the 9th day of growth, the surface aerial mycelium disappeared, and the hyphae began to aggregate. Over time, the hyphae gradually transitioned from light yellow to brown (Fig. 1a). Following PCR amplification and sequencing, a 783 bp fragment was obtained from strain ZS-1. The sequence was deposited in the GenBank database and assigned the accession number MH814912. BLAST sequence analysis of the ITS region using primers ITS1/ITS4 revealed that strain ZS-1 exhibited over 99% homology with multiple strains of *Rhizoctonia solani*. Notably, strain ZS-1 clustered together with the strain bearing accession number LC228062 of *R. solani* in the same clade, with a robust bootstrap confidence level of 100% (Fig. 1b). However, ZS-1 formed distinct branches separate from other Rhizoctonia species such as *Ceratobasidium oryzae-sativae*, *Rhizoctonia zeae*, and *Rhizoctonia cerealis*, as determined through sequence analysis and morphological observations. Consequently, the strain ZS-1, isolated from the infected zoysiagrass sample, was identified as *Rhizoctonia solani*.

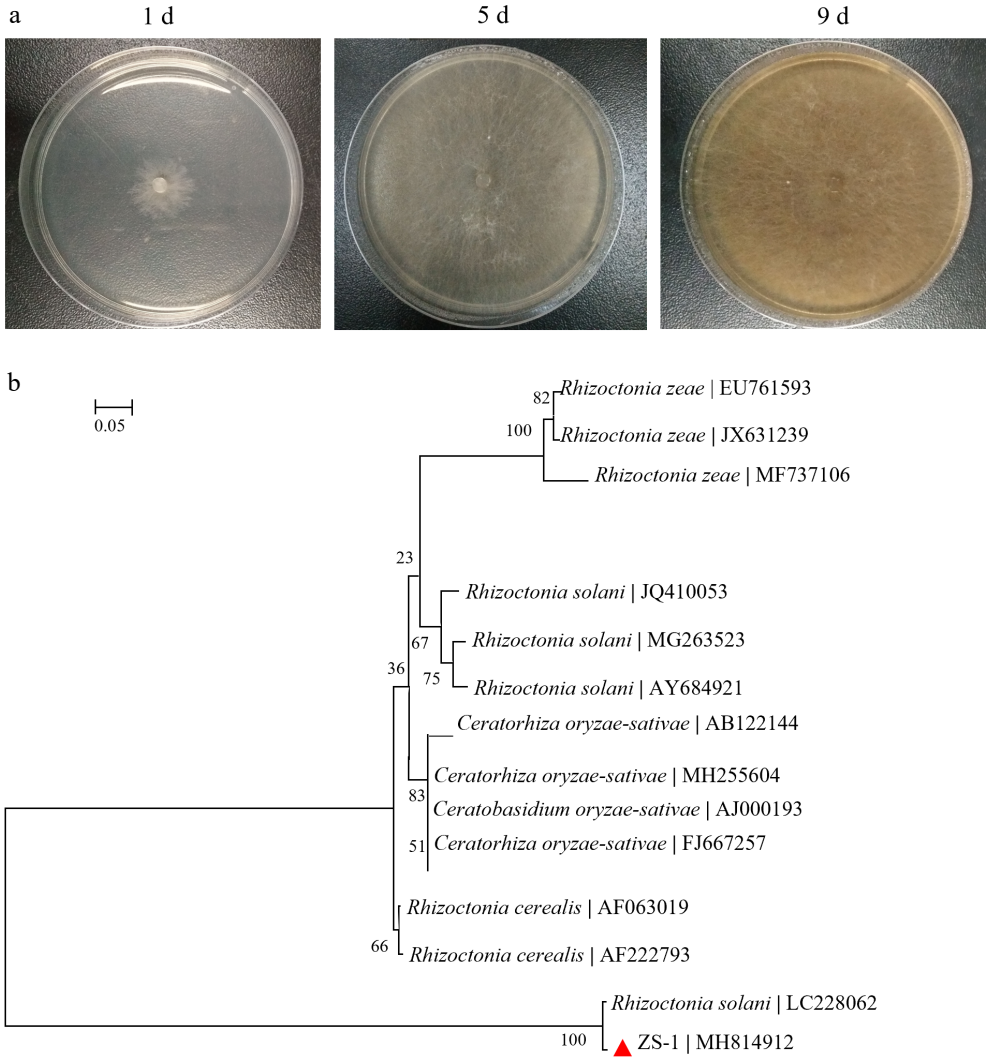

Fig. 1 (a) Colony morphology of the isolate ZS-1 on PDA causing Large Patch disease, and (b) phylogenetic tree of isolate ZS-1 and the related strains based on rDNA ITS sequences.

Determination of strain pathogenicity

Rhizoctonia solani ZS-1 was introduced through inoculation onto healthy zoysiagrass plants. Both disease incidence and severity index demonstrated significant temporal escalation ($p < 0.01$), specifically at 4, 8, and 12 d following inoculation. After 12-d of inoculation, the disease had a substantial impact, with the incidence rate (Fig. 2a), and severity index (Fig. 2b) in zoysiagrass reaching 71.67% and 52.73%, respectively.

The physiological response following inoculation of strain ZS-1 in zoysiagrass

In zoysiagrass subjected to LP treatment, several physiological parameters exhibited significant reductions when compared to HP treatment. Specifically, the turf quality, biomass, net photosynthetic rate (Pn), *Fv/Fm* (maximum quantum yield of PSII), photochemical quenching (qP), non-photochemical quenching (qN), the photosystem II Efficiency (ΦPSII), MDA levels, and EL all showed marked decreases under LP treatment (Fig. 3a–h, j, k; $p < 0.05$).

Furthermore, the chlorophyll and carotenoid content decreased in LP-treated zoysiagrass plants in comparison to HP-treated plants ($p < 0.05$; Fig. 3h, i). The chlorophyll and carotenoid contents were measured at 1.14 and 0.22 mg·g^{-1} FW in LP-treated plants, contrasting with 1.68 and 0.39 mg·g^{-1} FW in HP-treated plants.

Additionally, the activities of various defense enzymes, including SOD, POD, CAT, β-1,3-glucanase, and PAL activities, exhibited significant increases in LP-treated zoysiagrass plants when compared to their HP-treated counterparts ($p < 0.05$; Fig. 3l–p).

Changes in soil properties

Differences in soil nutrient levels between HP- and LP-treated zoysiagrass soil were observed to varying extents. In comparison to the HP treatment, the available phosphorus content in the rhizosphere soil was significantly higher in the LP treatment. Conversely, the available potassium, total nitrogen, total phosphorus, nitrate nitrogen, and organic matter content in the rhizosphere soil were significantly lower under the LP treatment. It's worth noting that the ammonium N (NH_4^+-N) content did not exhibit a significant difference between the two treatments (Supplementary Table S1).

Microbial diversity

The Venn diagrams derived from the rhizosphere operational taxonomic units (OTUs) analysis revealed that there was a total of 651 fungal OTUs shared between the HP and LP treatments. Among these, 483 fungal OTUs were unique to the HP treatment, and 256 fungal OTUs were unique to the LP treatment (Supplementary Fig. S1a). For bacteria, there were 1,880 bacterial OTUs shared between the HP and LP treatments, with 503 bacterial OTUs unique to the HP

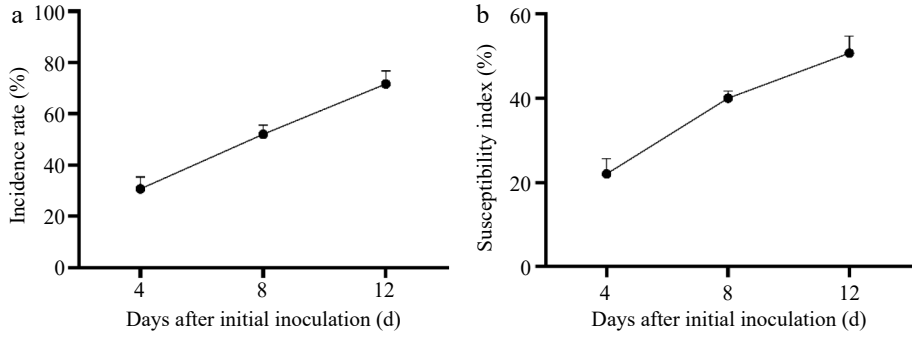

Fig. 2 (a) The incidence rate, and (b) severity index after ZS-1 strain invasion.

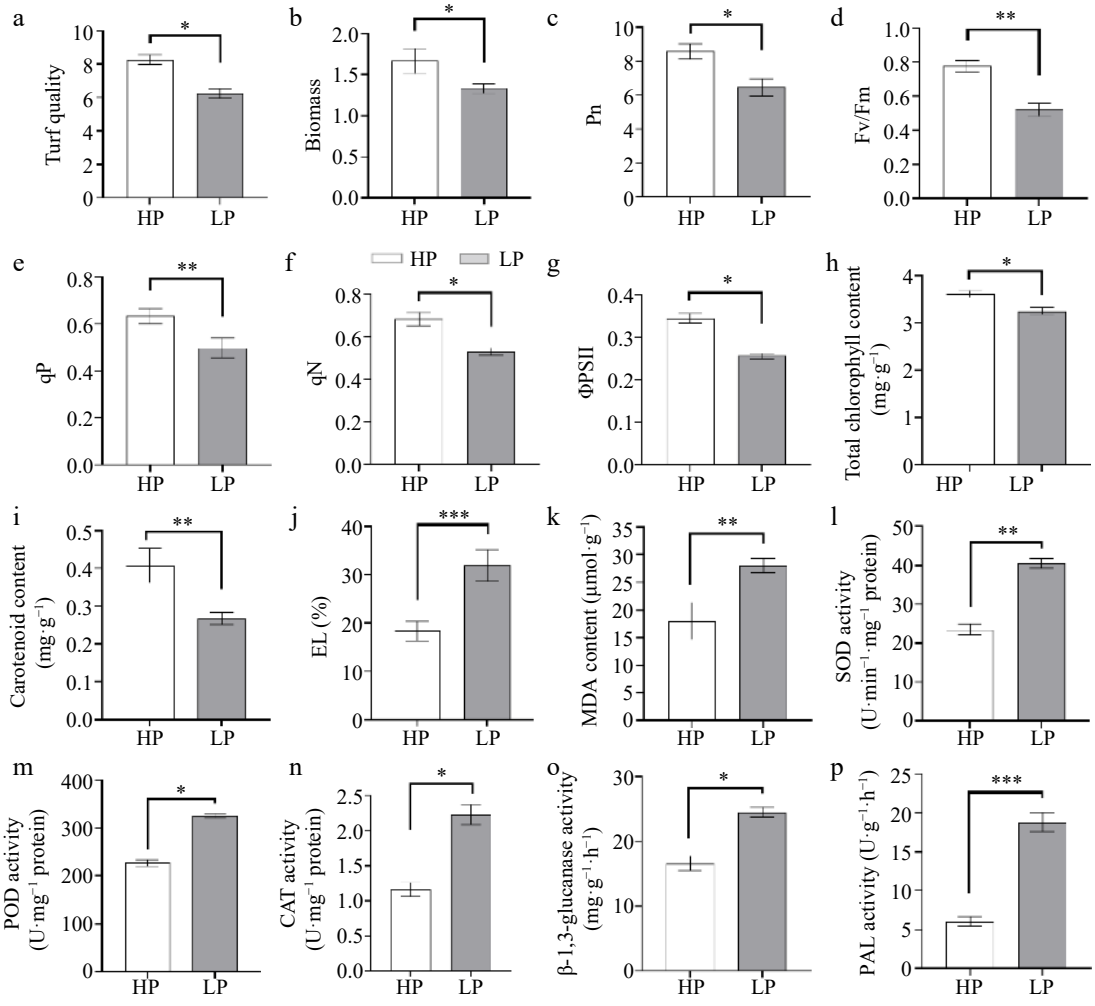

Fig. 3 Physiological indicators including (a) turf quality, (b) biomass, (c) net photosynthetic rate (Pn), (d) maximum quantum yield of PSII (Fv/Fm), (e) photochemical quenching (qP), (f) non-photochemical quenching (qN), (g) the photosystem II Efficiency (ΦPSII), (h) chlorophyll content, and (i) carotenoid content, (j) EL, (k) MDA level, (l) SOD, (m) POD, (n) CAT, (o) β-1,3-glucanase, and (p) PAL activities. (n = 3; 'LP' represents zoysiagrass grown with ZS-1 strain invasion; 'HP' represents zoysiagrass grown without ZS-1 strain invasion. '*', '**', '***', indicate significant differences at $p < 0.05$, $p < 0.01$, and $p < 0.001$, respectively).

treatment and 498 bacterial OTUs unique to the LP treatment (Supplementary Fig. S1b). Notably, the inoculation with *Rhizoctonia solani* ZS-1 had a reducing effect on the number of OTUs associated with rhizosphere fungi in zoysiagrass.

In the case of root-associated OTUs, the Venn diagrams indicated that there were 85 fungal OTUs common to both the HP and LP treatments, with 63 fungal OTUs unique to the HP treatment, and 28 fungal OTUs unique to the LP treatment (Supplementary Fig. S1c). For bacteria, 930 bacterial OTUs were shared between the HP and LP treatments, with 583 bacterial OTUs unique to the HP treatment and 366 bacterial OTUs unique to the LP treatment (Supplementary Fig. S1d). Similar to the fungal community, the inoculation with *Rhizoctonia solani* ZS-1 resulted in a reduction in the number of OTUs for both fungal and bacterial species associated with zoysiagrass roots.

Composition of the microbial community

In the rhizosphere, the relative abundance of fungal composition at the phylum level revealed that the highest proportions in the HP treatment were Ascomycota (70.76%), followed by Basidiomycota

(10.77%), Chytridiomycota (10.49%), and Glomeromycota (1.94%). In contrast, the LP treatment showed the top four relative abundances as Ascomycota (63.20%), Basidiomycota (13.01%), Chytridiomycota (14.09%), and Glomeromycota (4.62%) (Fig. 4a). At the genus level in the HP treatment, *Trichoderma* had the highest relative abundance (50.47%), followed by *Boothiomyces* (19.03%), *Staphylotrichum* (14.43%), *Penicillium* (8.46%), and *Hyalorbilia* (7.61%). In the LP treatment, the top genus in terms of relative abundance was *Trichoderma* (48.42%), followed by *Boothiomyces* (37.82%), *Penicillium* (8.96%), *Staphylotrichum* (4.23%), and *Hyalorbilia* (0.57%) (Fig. 4b).

For bacterial composition in the rhizosphere, at the phylum level, the highest relative abundance in the HP treatment was Proteobacteria (47.99%), followed by Actinobacteria (13.45%), Chloroflexi (9.12%), Bacteroidetes (9.10%), and Patescibacteria (5.06%). In the LP treatment, Proteobacteria accounted for the highest relative abundance at 43.62%, followed by Chloroflexi (14.39%), Actinobacteria

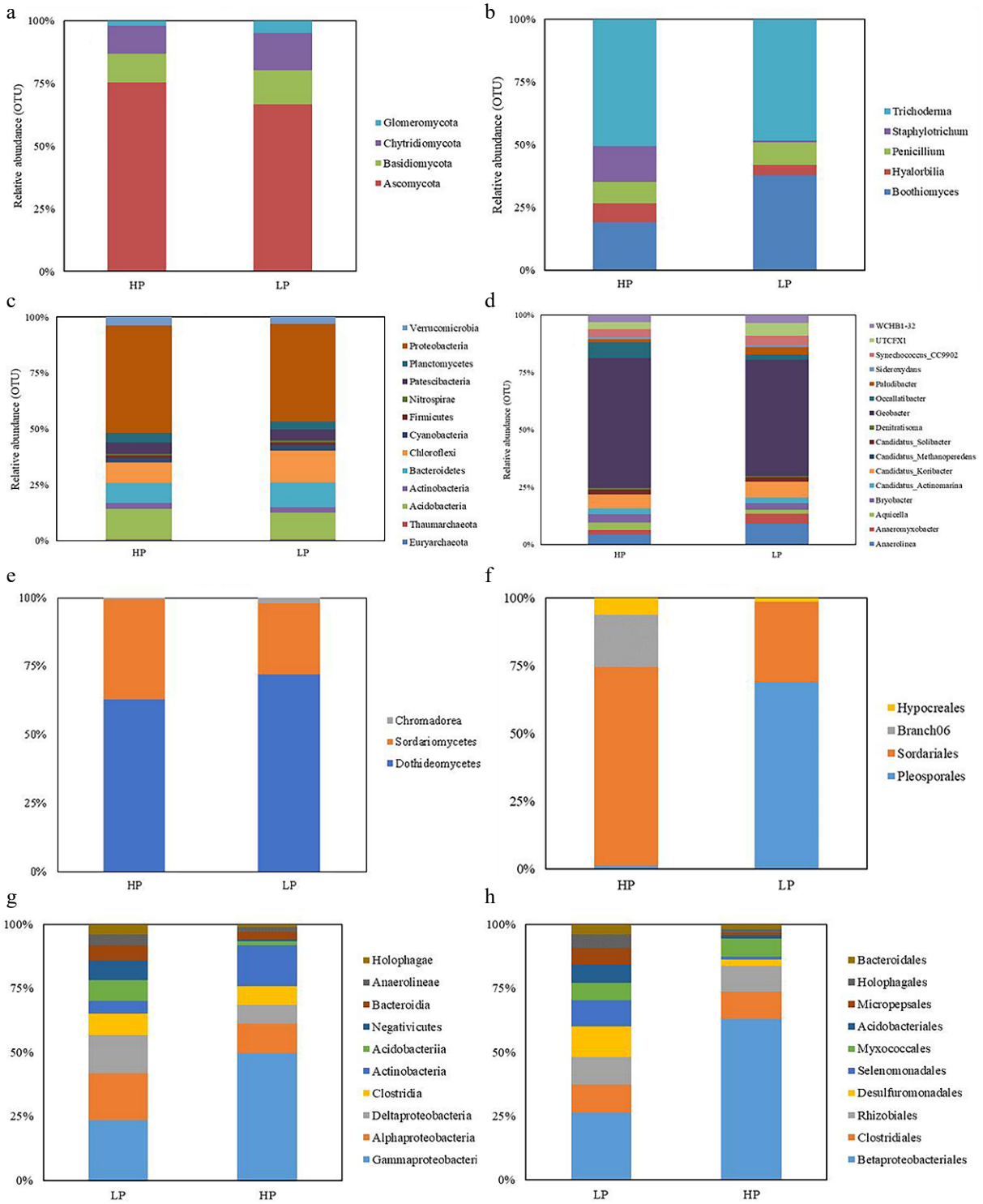

Fig. 4 The relative abundance of rhizosphere soil fungal (at the (a) phylum, and (b) genus level), and bacteria (at the (c) phylum, and (d) genus level) community as well as root fungal (at the (e) class, and (f) order level), and bacteria (at the (g) class, and (h) order level) community under ZS-1 strain invasion conditions. (n = 3; 'LP' represents zoysiagrass grown with ZS-1 strain invasion; 'HP' represents zoysiagrass grown without ZS-1 strain invasion).

(11.86%), Bacteroidetes (11.14%), and Patescibacteria (4.88%). At the genus level, the HP treatment displayed the highest relative abundance in the genus *Geobacter* (56.44%), followed by *Occallatibacter* (6.85%), *Candidatus_Koribacter* (6.02%), *Anaerolinea* (4.52%), and *Bryobacter* (3.71%) (Fig. 4c). In the LP treatment, the genus *Geobacter* had the highest relative abundance (50.57%), followed by *Anaerolinea* (9.32%), Candidatus_Koribacter (6.90%), UTCFX1 (5.59%), and Synechococcus_CC9902 (4.32%) (Fig. 4d).

Regarding the microbial community composition of zoysiagrass roots, the analysis focused on fungal and bacterial taxa with relative abundances exceeding 0.5% at the phylum and order levels. In terms of fungi, at the class level, the HP treatment had the highest relative abundance of Dothideomycetes (62.90%), followed by Sordariomycetes (36.36%), and Chromadorea (0.75%). The LP treatment also displayed a high relative abundance of Dothideomycetes (71.89%), followed by Sordariomycetes (25.96%), and Chromadorea (2.15%) (Fig. 4e). At the order level in the HP treatment, Sordariales was the most abundant (71.73%), followed by Branch06 (18.93%), Hypocreales (6.01%), and Pleosporales (1.18%). In the LP treatment, Pleosporales had the highest relative abundance (66.86%), followed by Sordariales (29.06%), and Hypocreales (1.43%) (Fig. 4f).

For bacteria, at the class level, the HP treatment exhibited the highest relative abundance of Gammaproteobacteria (49.77%), followed by Actinobacteria (15.89%), Alphaproteobacteria (11.47%), Clostridia (7.39%), and Deltaproteobacteria (7.29%). In the LP treatment, Gammaproteobacteria had the highest relative abundance (23.42%), followed by Alphaproteobacteria (18.29%), Deltaproteobacteria (15.04%), Clostridia (8.27%), and Acidobacteriia (8.07%) (Fig. 4g). At the order level in the HP treatment, Betaproteobacteriales had the highest relative abundance (62.89%), followed by Clostridiales (10.78%), Rhizobiales (7.95%), Myxococcales (6.68%), and Desulfuromonadales (2.69%). In the LP treatment, Betaproteobacteriales remained the highest, albeit decreased to 26.38% compared to the HP treatment. It was followed by Desulfuromonadales (12.06%), Clostridiales (11.00%), Rhizobiales (10.78%), and Selenomonadales (10.15%) (Fig. 4h).

Alpha diversity

Alpha diversity index results showed that inoculation with *R. solani* ZS-1 treatment significantly reduced ($p < 0.05$) the Chao1 index of rhizosphere and root fungal communities as well as root fungal communities (Fig. 5a–c), but significantly increased ($p < 0.01$) the Chao1 index of root bacterial communities (Fig. 5d). *R. solani* ZS-1 inoculation significantly reduced ($p < 0.05$) the Shannon index of both the rhizosphere and root fungal communities (Fig. 5e, g), while significantly increasing the Shannon index of both the rhizosphere and root bacterial communities (Fig. 5f, h). Contrasting with alpha diversity trends, Simpson indices exhibited inverse response patterns. The Simpson index of the rhizosphere and root fungal communities in the HP treatment was significantly lower ($p < 0.05$) than that in the LP treatment (Fig. 5i, k), while the Simpson index of its bacterial community in rhizosphere was significantly higher ($p < 0.05$) than that in the LP treatment (Fig. 5j), and the Simpson index of bacterial communities within the HP and LP root samples did not exhibit a significant difference ($p > 0.05$; Fig. 5l).

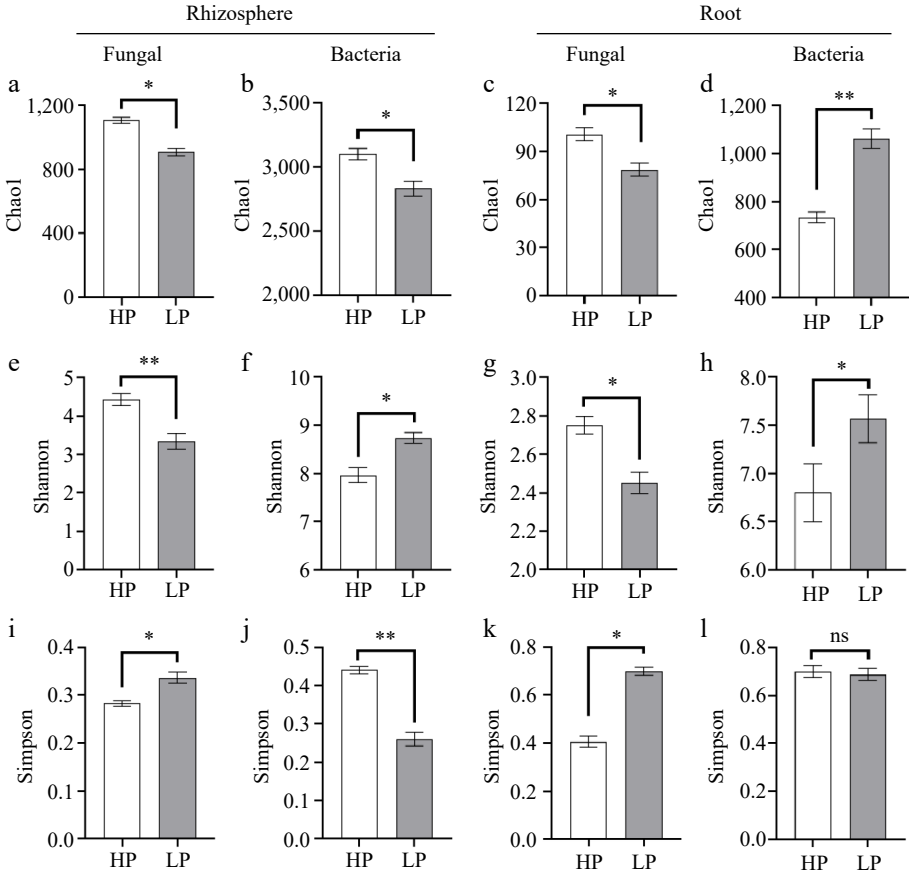

Fig. 5 Alpha diversity. Fungal and bacterial diversity and richness in rhizosphere soil and root. (a) Chao1, (e) Shannon, and (i) Simpson index of fungi in rhizosphere soil; (b) Chao1, (f) Shannon, and (j) Simpson index of bacteria in rhizosphere soil; (c) Chao1, (g) Shannon, and (k) Simpson index of fungi in root; (d) Chao1, (h) Shannon, and (l) Simpson index of bacteria in root. Bars denote means ± SE. (n = 3; 'LP' represents zoysiagrass grown with ZS-1 strain invasion; 'HP' represents zoysiagrass grown without ZS-1 strain invasion. '*', '**', indicate significant differences at $p < 0.05$, and $p < 0.01$, respectively and 'ns' represents no significant difference).

Beta diversity

For rhizosphere soil fungi and bacteria, PCoA plots showed different clusters for the LP and HP treatments (PCoA1 and PCoA2 explained 76.8% and 8.9% of the variance for fungi, and PCoA1 and PCoA2 explained 61.9% and 20.9% of the variance for bacteria, respectively) (Supplementary Fig. S2a, b). For root fungi and bacteria, PCoA plots showed different clusters for the LP and HP treatments (PCoA1 and PCoA2 explained 55.3% and 20.5% of the variance for fungi, and PCoA1 and PCoA2 explained 62.8% and 12.2% of the variance for bacteria, respectively). (Supplementary Fig. S2c, d).

LEfSe

LEfSe analysis was conducted to examine the effects of traffic treatment on zoysiagrass (from phylum to genus); their LDA scores were greater than 4.0. The longer the length of the column, the more apparent the differences between the species. For rhizosphere fungal community, *Staphylotrichum*, Chaetomiaceae, and unidentified (five unidentified species were present in this result) of HP treatment, Rhizophydiales, Terramycetaceae, *Boothiomyces*, Chytridiomycetes, Agaricales, Dothideomycetes, Basidiomycota, and Agaricomycetes of LP treatment (Fig. 6a). For rhizosphere bacterial community, Proteobacteria, Geobacteraceae, *Geobacter*, Desulfuromonadales, Deltaproteobacteria, *Occallatibacter*, Alphaproteobacteria, Acidobacteriaceae_Subgroup_1_, Diplorickettsiales, Diplorickettsiaceae, Phycisphaerae, and Tepidisphaerales of HP treatment, *Anaerolineae*, Chloroflexi, Anaerolineaceae, Anaerolineales, *Anaerolinea*, Bacteroidetes, Bacteroidales, Betaproteobacteriales, Rhodocyclaceae, and Archangiaceae of LP treatment (Fig. 6b). For root fungal community, Sordariomycetes, unidentified, Branch 06, unidentified, Branch06_sp, Magnaporthales, Magnaporthiopsis_sp, *Magnaporthiopsis*, Magnaporthaceae of HP treatment, Chromadorea, *Acrobeloides*, and Acrobeloides_sp of LP treatment (Fig. 6c). For root bacterial community, Actinobacteria, Proteobacteria, Gammaproteobacteria, Betaproteobacteriales, Burkholderiaceae, and Actinobacteria of HP treatment, Acidobacteria, Bacteroidetes, Spirochaetes, Deltaproteobacteria of LP treatment (Fig. 6d).

Redundancy analysis

The first and second RDA axes among rhizosphere soil fungal communities and plant indicators contributed 44.20% and 15.92% to the variance. The CAT activity was positively correlated with phyla Ascomycota, Anthophyta, Basidiomycota, Ciliophora, and Chytridiomycota. PAL activity was positively related to phyla Glomeromycota (Fig. 7a). The first and second RDA axes among rhizosphere soil bacterial communities and plant indicators contributed 62.29% and 12.67% to the variance. The CAT activity was positively correlated with phyla Actinobacteria and Acidobacteria. PAL activity was positively related to phyla Cyanobacteria, Bacteroidetes, and Chloroflexi (Fig. 7b).

The first and second RDA axes among root soil fungal communities and plant indicators contributed 86.46% and 10.28% to the variance. The CAT activity was positively correlated with Sordariales, Branch06, Sordariomycetes, and Dothideomycetes. PAL activity was positively related to Chromadorea (Fig. 7c). The first and second RDA axes among root soil bacterial communities and plant indicators contributed 99.11% and 0.09% to the variance. The CAT activity was positively correlated with Gammaproteobacteria. PAL activity was positively related to Deltaproteobacteria, Alphaproteobacteria, Clostridia, and Actinobacteria (Fig. 7d).

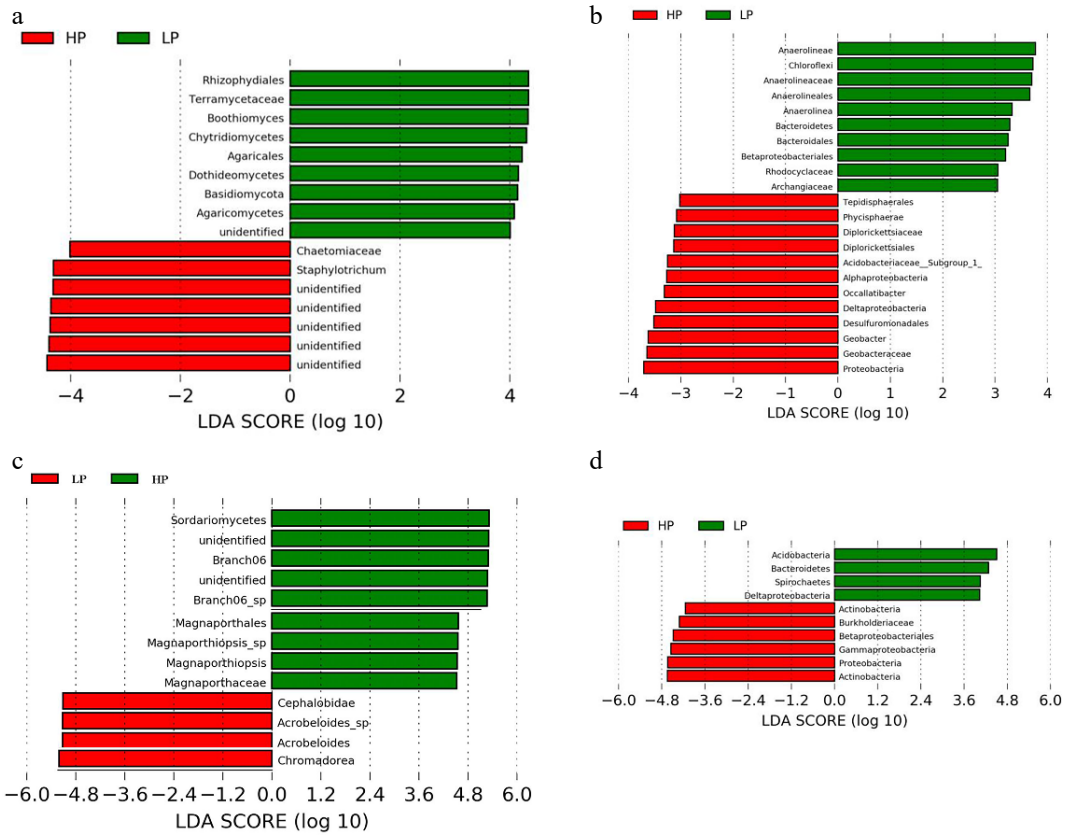

Fig. 6 The taxonomic differences between treatments based on ZS-1 strain invasion in zoysiagrass. Linear discriminant analysis Effect Size (LEfSe) of fungi and bacteria in (a), (b) rhizosphere soil, and (c), (d) root. LEfSe map is a linear discriminant analysis based on the composition of sample taxonomy according to different grouping conditions. $p < 0.05$, LDA > 4 as the standard. ('LP' represents zoysiagrass grown with ZS-1 strain invasion; 'HP' represents zoysiagrass grown without ZS-1 strain invasion).

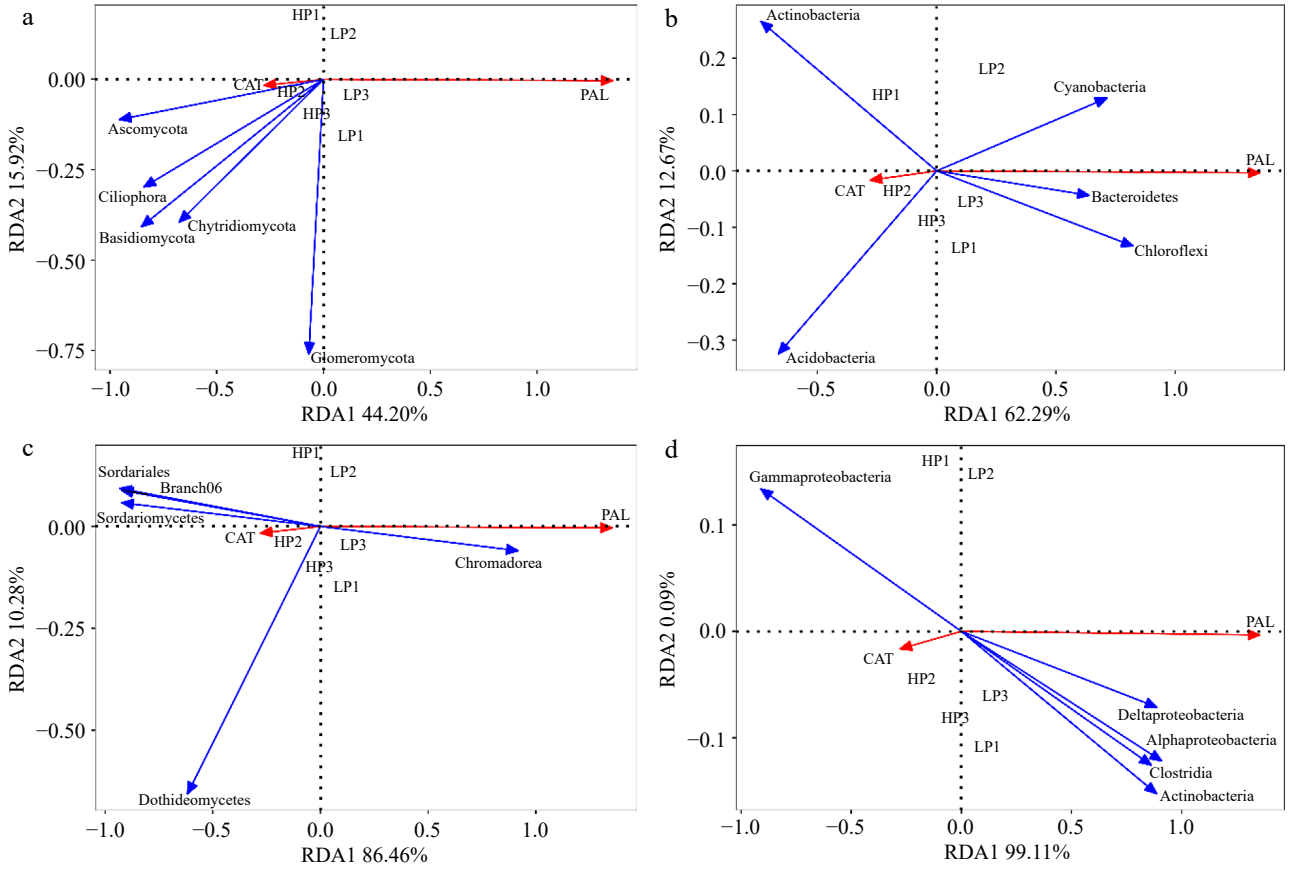

Fig. 7 Redundancy analysis (RDA) of relative abundance of fungi and bacteria in rhizosphere soil and root. and physiological indicators. (a) RDA between relative abundance of fungi in rhizosphere soil and physiological indicators; (b) RDA between relative abundance of bacteria in rhizosphere soil and physiological indicators; (c) RDA between relative abundance of fungi in root and physiological indicators; (d) RDA between relative abundance of bacteria in root and physiological indicators. (n = 3; 'LP' represents zoysiagrass grown with ZS-1 strain invasion; 'HP' represents zoysiagrass grown without ZS-1 strain invasion. CAT = catalase activity; PAL = phenylalanine ammonia-lyase activity).

The first and second RDA axes among rhizosphere soil fungal communities and soil properties contributed 83.99% and 12.27% to the variance. The AK and TP were positively correlated with phyla Glomeromycota. TN and TP were positively related to phyla Ciliophora, Ascomycota, and Basidiomycota (Fig. 8a). The first and second RDA axes among rhizosphere soil bacterial communities and soil properties contributed 83.68% and 11.82% to the variance. The AK was positively correlated with Bacteroidetes, Chloroflexi, and Cyanobacteria. TN and TP were positively related to Actinobacteria (Fig. 8b).

The first and second RDA axes among root soil fungal communities and soil properties contributed 86.44% and 7.05% to the variance. The AK was positively correlated with Chromadorea. TN and TP were positively related to Branch06, Sordariales, and Sordariomycetes (Fig. 8c). The first and second RDA axes among root soil bacterial communities and soil properties contributed 98.89% and 0.37% to the variance. The AK was positively correlated with Clostridia, Actinobacteria, Alphaproteobacteria, and Deltaproteobacteria. TN and TP were positively related to Gammaproteobacteria (Fig. 8d).

Discussion

Large Patch is the primary threat to the quality of zoysiagrass lawns. In our study, the invasion of the ZS-1 strain had adverse effects on the growth of zoysiagrass. Parameters such as Pn, Fv/Fm ratio, ΦPSII, qP, qN, chlorophyll, and carotenoid contents showed significant decreases in the LP treatment group (Supplementary Table S1). Simultaneously, the plant's defense mechanisms against pathogens were activated, as indicated by the significant increases in SOD, POD, CAT, APX, PAL, PPO, Chitinase, and β-1,3-glucanase activities in LP-treated zoysiagrass plants compared to their HP-treated counterparts. In addition, the LP treatment significantly reduced AK content in rhizosphere soil, which was positively correlated with CAT activity, consistent with previous research findings that potassium deficiency suppresses antioxidant enzyme activities[25].

Therefore, there is an urgent need to mitigate the impact of Large Patch disease on zoysiagrass turf. Currently, the incomplete genome sequencing of zoysiagrass and the challenges associated with genetic transformation have hindered molecular research and genetic engineering in zoysiagrass to some extent. It has been reported that rhizosphere-associated microorganisms can influence a plant's disease resistance mechanisms[26]. Investigating the colonization of microbial communities, followed by the screening and inoculation of beneficial bacteria or fungi, maybe a practical and meaningful strategy to alleviate the impact of Large Patch disease on zoysiagrass turf quality. In our current work, we assessed the diversity of rhizosphere and root-associated microbial communities in zoysiagrass under the invasion of the ZS-1 strain and under normal conditions using high-throughput sequencing of the 16S rRNA gene. At the phylum level, our findings revealed an increase in Chytridiomycota in rhizosphere samples under LP treatment, while Ascomycota and Basidiomycota consistently had the highest

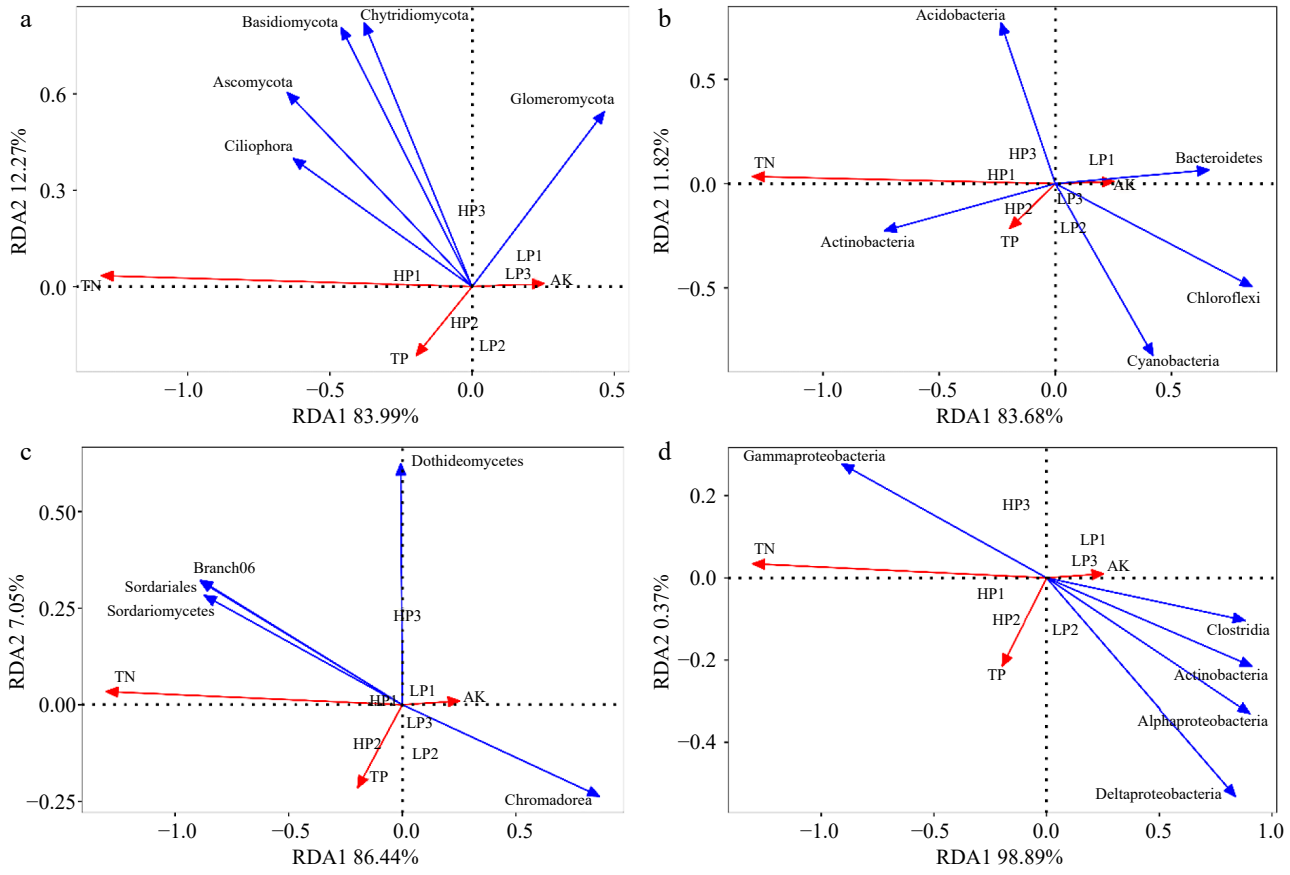

Fig. 8 Redundancy analysis (RDA) of relative abundance of fungi and bacteria in rhizosphere soil and root, and soil properties. (a) RDA between relative abundance of fungi in rhizosphere soil and soil properties; (b) RDA between relative abundance of bacteria in rhizosphere soil and soil properties; (c) RDA between relative abundance of fungi in root and soil properties; (d) RDA between relative abundance of bacteria in root and soil properties. (n = 3; 'LP' represents zoysiagrass grown with ZS-1 strain invasion; 'HP' represents zoysiagrass grown without ZS-1 strain invasion. AK = available potassium; TN = total nitrogen; TP = total phosphorus).

relative abundance in both LP and HP treatments. There were minor fluctuations in the relative distribution of species in the rhizosphere fungal community at different taxonomic levels. The phyla Ascomycota and Basidiomycota are the two major branches of soil fungi, primarily distributed in tropical and subtropical regions[27]. The reason why these two phyla, Ascomycota and Basidiomycota, are more abundant in tropical and subtropical soil compared to other fungal phyla is that they can produce regular septa with central pores that can be sealed to prevent leakage, thereby improving water conservation under dry conditions. This adaptation makes them more suitable for survival in low-latitude regions[28].

Taxonomic analysis revealed that the fungal community structure in zoysiagrass rhizosphere soils was primarily composed of genera such as *Trichoderma*, *Boothiomyces*, *Staphylotrichum*, and *Penicillium* under both HP and LP conditions. *Trichoderma* species are widely distributed across various climatic zones and play a significant role in decomposing woody and herbaceous materials. They are known for their rapid growth, ability to utilize diverse substrates and production of antimicrobial compounds. Recent studies have demonstrated that *Trichoderma* spp. can establish synergistic interactions with AMF, enhancing their biocontrol efficacy through joint secretion of antifungal metabolites[29]. *Trichoderma* strains have been utilized for enzyme and antibiotic production, bioremediation of xenobiotic substances, and as biological control agents against plant pathogenic fungi and nematodes. Some *Trichoderma* species can establish close associations with plant roots, contributing to biological control and promoting plant growth by releasing soluble mineral nutrients and growth-promoting compounds[30]. Both *Penicillium* and *Trichoderma* genera are considered to possess antifungal properties against plant pathogens[31,32]. Furthermore, the activity of catalase (CAT) was positively correlated with phyla such as Ascomycota, Anthophyta, Basidiomycota, Ciliophora, and Chytridiomycota. Phenylalanine ammonia-lyase (PAL) activity showed a positive relationship with the phylum Glomeromycota. Available potassium (AK) and total phosphorus (TP) are significantly positively correlated with the phylum Glomeromycota, which is consistent with previous studies showing that arbuscular mycorrhizal fungi (AMF) enhance stress resistance by promoting the uptake of potassium and phosphorus by host plants[33,34]. The total nitrogen (TN) and TP were positively correlated with phyla Ciliophora, Ascomycota, and Basidiomycota. Arbuscular mycorrhizal fungi (AMF), belonging to the Glomeromycotina subphylum, can form symbiotic relationships with approximately 80% of terrestrial plants. Some researchers suggest that mycorrhiza enhances plant disease resistance by improving plant nutrition, resulting in stronger growth and enhanced disease resistance[17,35]. There is indeed evidence that mycorrhizal plants tend to have higher phosphorus concentrations in their tissues compared to non-mycorrhizal plants. Some studies have found that the high phosphorus status within mycorrhizal roots reduces root exudates, thereby affecting the process of pathogen infection[36]. Arbuscular mycorrhizal (AM) fungi, like pathogens, are heterotrophic and require carbon nutrition from host plants. Competition for carbon resources by AM fungi reduces the opportunities for pathogens to acquire carbon, thus inhibiting

their growth and reproduction[37,38]. However, the specific mechanisms of this interaction are not yet fully understood. AM fungi and pathogens compete for infection sites or entry points. Once plant roots are colonized by AM fungi, it becomes challenging for pathogens to infect the roots. It has been observed that the pathogenic fungus *Rhizoctonia solani* struggles to infect maize roots that have been previously colonized by *Glomus mosseae* or *Glomus versiforme*, whereas maize roots without AM fungal colonization are more susceptible to *R. solani* infection[39]. AM fungi also interact with other antagonistic microorganisms in the rhizosphere, such as fungi like *Trichoderma* spp. and *Gliocladium* spp., as well as plant growth-promoting rhizobacteria (PGPR) like *Pseudomonas* spp. and *Bacillus* spp., resulting in mutualistic relationships. Increasing the diversity and abundance of beneficial microorganisms in the rhizosphere can reduce the chances of plant infection by pathogens, which could be one of the mechanisms through which AM fungi enhance plant disease resistance[40–42]. Therefore, these ZS-1 strain-induced AM fungi may interact with other microorganisms like *Trichoderma*, regulating plant physiology and specific mechanisms to promote zoysiagrass growth and enhance its resistance to Large Patch disease. However, further research is needed to fully understand these interactions.

In soil ecosystems, bacterial communities display a wide range of species abundances, with some species being present at low levels and a minority of species dominating the community. On a global scale, Proteobacteria and Acidobacteria are the predominant bacterial phyla in soils. In our study, we observed that Acidobacteria and Proteobacteria were the dominant phyla in soil samples from both HP and LP treatments, together accounting for approximately 50% of the total bacterial species in the soil samples. Proteobacteria play vital roles in nutrient recycling, promoting plant growth, and enhancing soil fertility. It has been suggested that copiotrophic bacteria, including some Proteobacteria, thrive in nutrient-rich or nutrient-limited environments[43]. However, the presence of the ZS-1 strain invasion led to a decrease in soil organic carbon (SOC) content, potentially reducing the support for the growth of Proteobacteria. Furthermore, the phyla Chloroflexi and Actinobacteria displayed higher abundances in turf soils under LP conditions. This observation is consistent with the copiotroph/oligotroph hypothesis[44], positing that bacterial phyla with oligotrophic traits predominantly occur in nutrient-impoverished environments. Taxonomic analysis has revealed that the bacterial community structure in zoysiagrass rhizosphere soils, both under high phosphorus (HP) and low phosphorus (LP) conditions, is predominantly comprised of genera *Geobacter*, *Candidatus_Koribacter*, and *Anaerolinea*. *Geobacter* species are widely distributed in soils and sediments and play significant roles in various environmental processes. They are involved in global carbon and iron cycles, contribute to bioremediation efforts by facilitating the cleanup of contaminants, and participate in diverse microbial processes. *Geobacter* species are particularly known for their ability to engage in direct electron transfer and syntrophic relationships with other microorganisms, impacting processes such as methane generation, nitrate reduction, and anaerobic photosynthesis within different microbial communities[45]. Bacteroidetes play crucial roles in recycling organic matter. Combined with the RDA result, The AK was positively correlated with Bacteroidetes, Chloroflexi, and Cyanobacteria. TN and TP were positively related to Actinobacteria, and they have been shown elsewhere to be associated with soils with nutrient deficiency[43]. Additionally, the fractions of dissolved organic matter (DOM) containing lignin-like and lipid-like compounds were strongly correlated with *Anaerolinea*, contributing to net nitrogen mineralization and SOC. Therefore, the rhizobacteria induced by the ZS-1 strain, particularly *Geobacter* and *Anaerolinea*, may enhance zoysiagrass growth and improve tolerance to Large Patch disease through specific mechanisms like enhancing the nitrogen cycle, nutrient uptake, and detoxification of harmful substances as plant growth-promoting rhizobacteria (PGPRs). While our correlation analysis suggests potential mechanisms, targeted metatranscriptomics is required to dissect causal relationships.

Microbial community restructuring may not only affect plant physiology but also feedback into soil chemistry via altered nutrient cycling (Supplementary Table S1). The interactions between microorganisms, soil, and plants play a crucial role in shaping the composition of underground microbial communities and ensuring ecosystem functionality. These interactions ultimately determine the normal growth of plants[46,47]. Therefore, when plants are exposed to soil-borne diseases, the microbial communities within the soil and root systems undergo varying degrees of change[48]. Such microbial shifts may represent an evolutionary conserved plant defense strategy. Through continuous evolution and adaptation, certain microorganisms may emerge to resist disease-causing pathogens, thereby ensuring that plants can continue to grow under similar conditions. Venn diagrams provide a visual representation of shared and unique information among multiple samples at a specific classification level. In this study, the number of fungal and bacterial OTUs (Operational Taxonomic Units) in HP samples from zoysiagrass rhizosphere soil was relatively high and comparable. However, in LP samples, the number of bacterial OTUs was significantly higher than the number of fungal OTUs. Analysis of shared OTUs between fungal and bacterial communities revealed that the number of shared OTUs in bacterial communities between HP and LP samples was significantly higher than in fungal communities. Additionally, in both root and rhizosphere communities, the number of bacterial OTUs was significantly higher than the number of fungal OTUs. Furthermore, the number of shared OTUs was significantly higher in bacterial communities compared to fungal communities. Research, such as Coleman-Derr et al.[49], on the rhizosphere microbiome of *Arabidopsis thaliana* has shown that plant roots have a selective filtering effect on the microorganisms that colonize within them. Root secretions can attract microorganisms from the surrounding soil, and after undergoing selection, these microorganisms can colonize the plant roots. In the root samples of zoysiagrass, at the class level, in HP samples, the highest relative abundance of fungi was observed in the class Dothideomycetes with a relative abundance of up to 62.90%. At the order level, *Sordariales* had a notably high relative abundance of approximately 71.73%. In LP samples, Dothideomycetes still maintained the highest relative abundance, approximately 71.89%, while at the order level, *Pleosporales* dominated with a relative abundance of around 66.86%. *Pleosporales* has been reported to exhibit resistance to pathogens[50]. The CAT activity, TN (total nitrogen), and TP (total phosphorus) showed positive correlations with *Sordariales*, *Branch06*, and *Sordariomycetes*. It's worth noting that *Sordariales* includes several thermophilic taxa associated with the production of thermostable enzymes[51]. Additionally, CAT activity was positively correlated with *Gammaproteobacteria*. PAL activity exhibited positive associations with *Deltaproteobacteria*, *Alphaproteobacteria*, *Clostridia*, and Actinobacteria. AK (available potassium) was positively correlated with *Clostridia*, Actinobacteria, *Alphaproteobacteria*, and *Deltaproteobacteria*. TN and TP were positively related to *Gammaproteobacteria*. *Deltaproteobacteria* has been implicated in sulfur oxidation and carbon fixation[52], while *Clostridia* play a role in nutrient metabolism.

Hence, these beneficial microorganisms induced by the ZS-1 strain in the rhizosphere soil and within the roots may enhance zoysiagrass growth and improve its resistance to diseases through

specific mechanisms such as enhancing nitrogen cycling, nutrient uptake, and modulating plant physiology. While 16S/ITS sequencing identified key taxa, their functional gene expression and metabolic flux require multi-omics integration. Subsequent studies should combine *Geobacter* isolation with gnotobiotic systems to validate disease-suppressive roles. The interactions between rhizosphere and root-associated bacterial communities could potentially contribute to enhancing plant resilience[53]. Additionally, during the ZS-1 strain invasion process, robust fundamental biological processes, replication, recombination, and repair in both rhizosphere soil and plant roots may also play a role in improving zoysiagrass resilience[4]. In future studies, we plan to cultivate and inoculate beneficial microorganisms in rhizosphere soil, while also analyzing the relationship between zoysiagrass disease resistance, physiological and biochemical processes, and soil microbial communities. Indeed, managing rhizosphere and root microbes and ensuring a balanced composition of beneficial and harmful microbes in the soil and around plant roots is a crucial aspect of enhancing plant resilience to both abiotic and biotic stresses.

Conclusions

This study first reveals that *R. solani* exacerbates disease progression by reshaping rhizosphere-root microbiome networks, identifying novel microbial targets (e.g., *Geobacter-Anaerolinea* functional modules) for turfgrass disease management. However, it's important to note that this study provides preliminary findings and focuses solely on the interaction between the pathogenic ZS-1 strain and the plant host. Further research involving additional microorganisms is necessary to comprehensively analyze their potential roles in mitigating Large Patch disease. This research contributes to a better understanding of the symbiotic relationship between dominant microbial communities and zoysiagrass, laying the foundation for future efforts aimed at improving zoysiagrass resistance to Large Patch through enhancements in soil microbial community and microbial colonization within the roots.

Author contributions

The authors confirm contribution to the paper as follows: study conception and design: Zheng X, Liu T; data collection: Tang H, Wei H; analysis and interpretation of results: Zheng X, Tang H, Wei H, Liu W; draft manuscript preparation: Zheng X, Liu W. All authors reviewed the results and approved the final version of the manuscript.

Data availability

All data generated or analyzed during this study are included in this published article and its supplementary information files.

Acknowledgments

This research was supported by Natural Science Foundation of Guangdong Province [NO. 2020A1515011261].

Conflict of interest

The authors declare that they have no conflict of interest.

Supplementary information accompanies this paper at (https://www.maxapress.com/article/doi/10.48130/grares-0025-0016)

Dates

Received 15 March 2025; Revised 26 April 2025; Accepted 7 May 2025; Published online 3 July 2025

References

1. Zhang J, Richardson M, Karcher D, McCalla J, Mai J, et al. 2021. Dormant sprigging of bermudagrass and zoysiagrass. *HortTechnology* 31:395–404
2. Bock EM, Easton ZM. 2020. Export of nitrogen and phosphorus from golf courses: a review. *Journal of Environmental Management* 255:109817
3. Kim YS, Lee KS, Kim HG, Lee GJ. 2022. Biocontrol of Large Patch disease in zoysiagrass (*Zoysia japonica*) by *Bacillus subtilis* SA-15: identification of active compounds and synergism with a fungicide. *Horticulturae* 8:34
4. Feng K, Zhang Y, He Z, Ning D, Deng Y. 2019. Interdomain ecological networks between plants and microbes. *Molecular Ecology Resources* 19:1565–77
5. Sykes VR, Horvath BJ, Warnke SE, Askew SD, Baudoin AB, et al. 2017. Comparing digital and visual evaluations for accuracy and precision in estimating tall fescue brown patch severity. *Crop Science* 57:3303–09
6. Hu L, Robert CAM, Cadot S, Zhang X, Ye M, et al. 2018. Root exudate metabolites drive plant-soil feedbacks on growth and defense by shaping the rhizosphere microbiota. *Nature Communications* 9:2738
7. Wei H, He W, Li Z, Ge L, Zhang J, et al. 2022. Salt-tolerant endophytic bacterium *Enterobacter ludwigii* B30 enhance bermudagrass growth under salt stress by modulating plant physiology and changing rhizosphere and root bacterial community. *Frontiers in Plant Science* 13:959427
8. Martin FM, Uroz S, Barker DG. 2017. Ancestral alliances: plant mutualistic symbioses with fungi and bacteria. *Science* 356:eaad4501
9. Galaviz C, Lopez BR, de-Bashan LE, Hirsch AM, Maymon M, et al. 2018. Root growth improvement of mesquite seedlings and bacterial rhizosphere and soil community changes are induced by inoculation with plant growth-promoting bacteria and promote restoration of eroded desert soil. *Land Degradation & Development* 29:1453–66
10. Baek D, Rokibuzzaman M, Khan A, Kim MC, Park HJ, et al. 2020. Plant-growth promoting *Bacillus oryzicola* YC7007 modulates stress-response gene expression and provides protection from salt stress. *Frontiers in Plant Science* 10:1646
11. Ji C, Wang X, Song X, Zhou Q, Li C, et al. 2021. Effect of *Bacillus velezensis* JC-K3 on endophytic bacterial and fungal diversity in wheat under salt stress. *Frontiers in Microbiology* 12:802054
12. Zamioudis C, Pieterse CMJ. 2012. Modulation of host immunity by beneficial microbes. *Molecular Plant-Microbe Interactions* 25:139–50
13. Lee K, Lee J, Kim G, Kim Y, Kang S, et al. 2017. Rough-surface-enabled capacitive pressure sensors with 3D touch capability. *Small* 13:1700368
14. Burgess P, Huang B. 2014. Growth and physiological responses of creeping bentgrass (A*grostis stolonifera*) to elevated carbon dioxide concentrations. *Horticulture Research* 1:14021
15. Murchie EH, Lawson T. 2013. Chlorophyll fluorescence analysis: a guide to good practice and understanding some new applications. *Journal of Experimental Botany* 64:3983–98
16. Lichtenthaler HK, Wellburn AR. 1983. Determinations of total carotenoids and chlorophylls *a* and *b* of leaf extracts in different solvents. *Biochemical Society Transactions* 11:591–92
17. Gao WQ, Lü LH, Srivastava AK, Wu QS, Kuča K. 2020. Effects of mycorrhizae on physiological responses and relevant gene expression of peach affected by replant disease. *Agronomy* 10:186
18. Wu W, Tang XP, Yang C, Liu HB, Guo NJ. 2013. Investigation of ecological factors controlling quality of flue-cured tobacco (*Nicotiana tabacum* L.) using classification methods. *Ecological Informatics* 16:53–61
19. Walkley A. 1935. An examination of methods for determining organic carbon and nitrogen in soils (with one text-figure.). *The Journal of Agricultural Science* 25:598–609
20. Caporaso JG, Kuczynski J, Stombaugh J, Bittinger K, Bushman FD, et al. 2010. QIIME allows analysis of high-throughput community sequencing data. *Nature Methods* 7:335–36

21. Quast C, Pruesse E, Yilmaz P, Gerken J, Schweer T, et al. 2013. The SILVA ribosomal RNA gene database project: improved data processing and web-based tools. *Nucleic Acids Research* 41:D590–D596
22. Wickham H. 2016. *ggplot2*. Cham: Springer International Publishing. doi: 10.1007/978-3-319-24277-4
23. McMurdie PJ, Holmes S. 2013. phyloseq: an R package for reproducible interactive analysis and graphics of microbiome census data. *PLoS One* 8:e61217
24. Oksanen J, Blanchet FG, Friendly M, Kindt R, Legendre P, et al. 2020. *vegan: community ecology package, version 2.5-7 November 2020*. http://CRAN.R-project.org/package=vegan
25. Zheng Y, Li Z, Tan Z, Liu Y, Zhang X, et al. 2025. Iron (II)-EDTA alleviate salinity injury through regulating ion balance in halophyte seashore *Paspalum*. *Grass Research* 5:e002
26. Yin C, Casa Vargas JM, Schlatter DC, Hagerty CH, Hulbert SH, et al. 2021. Rhizosphere community selection reveals bacteria associated with reduced root disease. *Microbiome* 9:86
27. Bastian F, Bouziri L, Nicolardot B, Ranjard L. 2009. Impact of wheat straw decomposition on successional patterns of soil microbial community structure. *Soil Biology and Biochemistry* 41:262–75
28. Beck J, Echtenacher B, Ebel F. 2013. Woronin bodies, their impact on stress resistance and virulence of the pathogenic mould *Aspergillus fumigatus* and their anchoring at the septal pore of filamentous Ascomycota. *Molecular Microbiology* 89:857–71
29. Bao X, Zou J, Zhang B, Wu L, Yang T, et al. 2022. Arbuscular mycorrhizal fungi and microbes interaction in rice mycorrhizosphere. *Agronomy* 12:1277
30. Hoyos-Carvajal L, Orduz S, Bissett J. 2009. Genetic and metabolic biodiversity of *Trichoderma* from Colombia and adjacent neotropic regions. *Fungal Genetics and Biology* 46:615–31
31. Kwaśna H, Łakomy P, Mallett K. 2004. Reaction of *Armillaria ostoyae* to forest soil microfungi. *Forest Pathology* 34:147–62
32. Fall AF, Nakabonge G, Ssekandi J, Founoune-Mboup H, Apori SO, et al. 2022. Roles of arbuscular mycorrhizal fungi on soil fertility: contribution in the improvement of physical, chemical, and biological properties of the soil. *Frontiers in Fungal Biology* 3:723892
33. Li J, Chai Q, Chen Z, Malik K, Li C. 2025. Interactions of Epichloë endophyte and arbuscular mycorrhizal fungi on wild barley under salt stress. *Grass Research* 5:e007
34. Bennett AE, Groten K. 2022. The costs and benefits of plant-arbuscular mycorrhizal fungal interactions. *Annual Review of Plant Biology* 73:649–72
35. Moukarzel R, Ridgway HJ, Liu J, Guerin-Laguette A, Jones EE. 2022. AMF community diversity promotes grapevine growth parameters under high black foot disease pressure. *Journal of Fungi* 8:250
36. Spagnoletti FN, Leiva M, Chiocchio V, Lavado RS. 2018. Phosphorus fertilization reduces the severity of charcoal rot (*Macrophomina phaseolina*) and the arbuscular mycorrhizal protection in soybean. *Journal of Plant Nutrition and Soil Science* 181:855–60
37. Ren L, Lou Y, Zhang N, Zhu X, Hao W, et al. 2013. Role of arbuscular mycorrhizal network in carbon and phosphorus transfer between plants. *Biology and Fertility of Soils* 49:3–11
38. Wang F, Zhang L, Zhou J, Rengel Z, George TS, et al. 2022. Exploring the secrets of hyphosphere of arbuscular mycorrhizal fungi: processes and ecological functions. *Plant and Soil* 481:1–22
39. Song YY, Cao M, Xie LJ, Liang XT, Zeng RS, et al. 2011. Induction of DIMBOA accumulation and systemic defense responses as a mechanism of enhanced resistance of mycorrhizal corn (*Zea mays* L.) to sheath blight. *Mycorrhiza* 21:721–31
40. Neeraj, Singh K. 2011. Organic amendments to soil inoculated arbuscular mycorrhizal fungi and *Pseudomonas fluorescens* treatments reduce the development of root-rot disease and enhance the yield of *Phaseolus vulgaris* L. *European Journal of Soil Biology* 47:288–95
41. Dehariya K, Shukla A, Sheikh I, Vyas D. 2015. *Trichoderma* and arbuscular mycorrhizal fungi based biocontrol of *Fusarium udum* butler and their growth promotion effects on pigeon pea. *Journal of Agricultural Science and Technology* 17:505–17
42. Devi NO, Tombisana Devi RK, Debbarma M, Hajong M, Thokchom S. 2022. Effect of endophytic *Bacillus* and arbuscular mycorrhiza fungi (AMF) against *Fusarium* wilt of tomato caused by *Fusarium oxysporum* f. sp. lycopersici. *Egyptian Journal of Biological Pest Control* 32:1
43. Beckers B, De Beeck MO, Weyens N, Boerjan W, Vangronsveld J. 2017. Structural variability and niche differentiation in the rhizosphere and endosphere bacterial microbiome of field-grown poplar trees. *Microbiome* 5:25
44. Fierer N, Bradford MA, Jackson RB. 2007. Toward an ecological classification of soil bacteria. *Ecology* 88:1354–64
45. Huang L, Liu X, Ye Y, Chen M, Zhou S. 2020. Evidence for the coexistence of direct and riboflavin-mediated interspecies electron transfer in *Geobacter* co-culture. *Environmental Microbiology* 22:243–54
46. Castiglione AM, Mannino G, Contartese V, Bertea CM, Ertani A. 2021. Microbial biostimulants as response to modern agriculture needs: composition, role and application of these innovative products. *Plants* 10:1533
47. Coban O, De Deyn GB, van der Ploeg M. 2022. Soil microbiota as game-changers in restoration of degraded lands. *Science* 375:abe0725
48. Altieri MA, Nicholls CI. 2003. Soil fertility management and insect pests: harmonizing soil and plant health in agroecosystems. *Soil and Tillage Research* 72:203–11
49. Coleman-Derr D, Desgarennes D, Fonseca-Garcia C, Gross S, Clingenpeel S, et al. 2016. Plant compartment and biogeography affect microbiome composition in cultivated and native *Agave* species. *New Phytologist* 209:798–811
50. Hongsanan S, Hyde KD, Phookamsak R, Wanasinghe DN, McKenzie EHC, et al. 2020. Refined families of Dothideomycetes: Dothideomycetidae and Pleosporomycetidae. *Mycosphere* 11:1553–2107
51. van den Brink J, Facun K, de Vries M, Stielow JB. 2015. Thermophilic growth and enzymatic thermostability are polyphyletic traits within Chaetomiaceae. *Fungal Biology* 119:1255–66
52. Langwig MV, De Anda V, Dombrowski N, Seitz KW, Rambo IM, et al. 2022. Correction to: Large-scale protein level comparison of Deltaproteobacteria reveals cohesive metabolic groups. *The ISME Journal* 16:899
53. Dai L, Zhang G, Yu Z, Ding H, Xu Y, et al. 2019. Effect of drought stress and developmental stages on microbial community structure and diversity in peanut rhizosphere soil. *International Journal of Molecular Sciences* 20:2265